Rimpilainen, T. E.; Alu, Andrea; Sihvola, Ari

Implementing radial anisotropy with self-similar structures

Implementing radial anisotropy with self-similar structures

T. E. Rimpiläinen[*] and A. Alù

Photonics Initiative, Advanced Science Research Center, City University of New York, 85 Saint Nicholas Terrace, New York, USA

A. Sihvola

Department of Electronics and Nanoengineering, Aalto University School of Electrical Engineering,
P.O. Box 15500, FI-00076, AALTO, Finland

Radial anisotropy in small objects has been linked to exotic optical properties. It can be implemented with a spherical inclusion that manifests self-similarity. We show that, when a self-similar, onion-like structure with alternating layers is homogenized by using an effective material approximation, the homogenized material becomes uniaxially anisotropic with the axis of anisotropy pointed radially outward from the center of the inclusion. This radial anisotropy becomes exact in the limit of a dense set of layers. The exact equivalence of the layered self-similar inclusion and the radially anisotropic inclusion manifests itself both in the effective permittivities of the two inclusions—when homogenized over the entire volumes—and in the internal potentials. Because the layered sphere and the radially anisotropic sphere are analogous, it is possible to study some of the interesting scattering features of radially anisotropic spheres in a realistic configuration. In particular, we show that the outcome of homogenizing the self-similar inclusion, and consequently the electric response, depends on what the core material at the center of the inclusion is and that a continuous transition between the two homogenization models is possible. The findings suggest intriguing applications in nanophotonics.

I. INTRODUCTION

Spherical inclusions that manifest *radial anisotropy* (RA) have been a focus of recent research because they support exotic interactions with light, including the possibility of cloaking an object or magnifying it [1–4], and because practical implementations of the inclusion exist [5,6]. In the electrostatic limit—i.e., when the object is much smaller than the wavelength—the material of the radially anisotropic sphere is sufficiently defined by its two permittivity components—the radial permittivity $\epsilon_\parallel$ and the tangential permittivity $\epsilon_\perp$—which are both constant throughout the volume of the inclusion (Fig. 1). The two components, $\epsilon_\parallel$ and $\epsilon_\perp$, define the uniaxial permittivity

$$\bar{\bar{\epsilon}} = \epsilon_\parallel \mathbf{u}_r \mathbf{u}_r + \epsilon_\perp (\bar{\bar{I}} - \mathbf{u}_r \mathbf{u}_r), \quad (1)$$

where $\mathbf{u}_r$ is the radial unit vector of the spherical coordinate system (r, θ, φ) that has its origin at the center of the inclusion. The anisotropy axis of the material varies between points, so that the preferred direction is always pointed in the direction of the local normal vector except in the singular point at the center of the inclusion where the axis of anisotropy is indeterminate.

The radially anisotropic sphere was first studied in its punctured form, where a spherical radially anisotropic coating is taken to envelop a homogeneous spherical core. The *punctured* radially anisotropic sphere was studied by Roth and

Dignam [7] (1973), who based their approach on Güttler's derivation for the locally homogeneous core-shell structure [8]. Schulgasser [9] (1983) discussed the *intact* radially anisotropic sphere, in which the homogeneous core is absent. This seminal work has been followed by research on the exotic scattering response of these structures [10–14]. In subsequent work, the spherical geometry has been generalized into a spheroidal one [15,16] and the uniaxial material has been generalized into biaxial [17,18]. Another flavor of radial anisotropy is the cylindrical anisotropy. Infinitely long cylinders with cylindrical anisotropy have been studied [19–21].

This article studies a way to implement the radially anisotropic sphere by using a set of layers that are both homogeneous and isotropic (Fig. 1). In this implementation, a uniaxial medium results when the layers are locally homogenized by using an effective medium approximation at some small neighborhood around each given point inside the inclusion. If the chosen neighborhoods are taken to be sufficiently small, the layers may be regarded as being planar within the given neighborhood. Furthermore, if the set of layers is sufficiently dense and sufficiently regular, the volume fractions of each specific type of layer or the total volume of the neighborhood are predictable.

The main contribution of this article consists in analytically solving the electrostatic problem that involves an onion-like, self-similar structure, consisting of an indefinitely dense set of infinitesimally thin layers (Fig. 1). The material parameter of the layers alternates between ϵ_1 and ϵ_2. In the given idealistic model, this alternating pattern is imagined to continue indefinitely toward the center of the inclusion. The fraction a_{n+1}/a_n between the outer radii of any subsequent spherical layers is
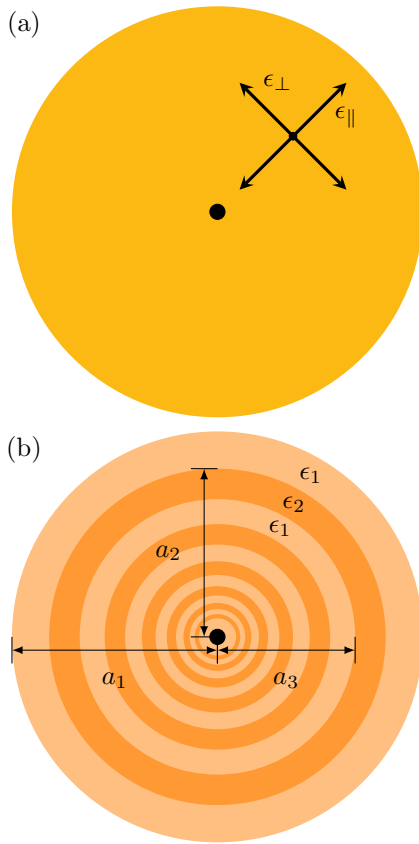
*t.rimpil00@ccny.cuny.edu

FIG. 1. (a) Radially anisotropic sphere and (b) its approximate implementation with a self-similar sphere. A radially anisotropic sphere results when a sufficiently dense layered structure is locally homogenized.

taken to have a fixed value within the whole set of layers. When the limit $a_{n+1}/a_n \to 1^-$ of vanishingly thin layers is taken, all finite domains inside the sphere contain material with ϵ_1 and material with ϵ_2 in equal proportions.

A homogenization may be performed locally, at each given small subdomain of the inclusion to establish an analogy between the radially anisotropic sphere in the upper panel of Fig. 1 and the self-similar sphere in the lower panel. The material of the inclusion may be locally modeled as consisting of a set of planar layers, alternating between the material parameters ϵ_1 and ϵ_2 so that the thickness of each layer remains constant throughout the entire volume. This local homogenization gives the values [22, Eq. 8.8–8.9]

$$\epsilon_\parallel = \frac{2\epsilon_1\epsilon_2}{\epsilon_1 + \epsilon_2}, \quad \epsilon_\perp = \frac{\epsilon_1 + \epsilon_2}{2} \quad (2)$$

to the parallel permittivity component $\epsilon_\parallel$ and the perpendicular permittivity component $\epsilon_\perp$ of the anisotropic permittivity $\bar{\bar{\epsilon}}$ in Eq. (1). It seems clear that, when the two kinds of components of the material parameters are related by Eq. (2), the local homogenization establishes an analogy between a given radially anisotropic sphere and the corresponding self-similar sphere. Our goal is to rigorously prove this analogy.

We establish the analogy in two parts. First, we show that the radially anisotropic sphere and the self-similar sphere have the same electrostatic response outside the sphere. The

electrostatic response of the radially anisotropic sphere is characterized by its *effective permittivity*, which is the effective permittivity of the inclusion when a homogenization is performed over the entire inclusion, i.e., not merely over a small local subdomain, like above. The effective permittivity of a radially anisotropic sphere is known in the literature [4] and is

$$\epsilon_{\mathrm{eff}} = \frac{\epsilon_\parallel}{2} \left(\pm\sqrt{1 + 8\frac{\epsilon_\perp}{\epsilon_\parallel}} - 1 \right). \quad (3)$$

Despite the local anisotropy of the material, the inclusion as a whole is isotropic because of its spherical symmetry. Therefore, a simple scalar quantity suffices to represent the effective permittivity. When we, in Sec. III A, derive the effective permittivity of the self-similar sphere, we again arrive at Eq. (3), proving that the effective permittivities are the same. Second, in Sec. III C, we show that the internal potentials of the self-similar sphere and the radially anisotropic sphere coincide.

A few approaches on the implementation of radial anisotropy have been discussed in the literature [5,9,19]. In particular, Mangini *et al.* [6] discussed an implementation that uses a set of equidistant layers—keeping the layer thickness $a_n - a_{n+1}$ rather than the fraction a_{n+1}/a_n fixed between the layers. The advantage of the presently introduced method, which keeps the radius fraction fixed, is that the chosen implementation allows one to explicitly use the self-similarity of the onion-like structure as a tool for analysis. Also, the chosen implementation does not approximate radial anisotropy less accurately near the center of the inclusion than near the surface, as is the case with a structure of uniformly thick layers.

The method that is presented in this article is conceptually similar to the way in which an infinite geometric series may be evaluated by employing its self-similarity. For a geometric series $s = \Sigma q^n$, there exists a nontrivial function $f(s) = 1 + qs$ that leaves the series unchanged. We then refer to the value of the sum as the *fixed point* of the function. The fixed-point condition $f(s) = s$, when solved for s, gives the value of the series, $s = 1/(1 - q)$.

In the same way, it follows from the self-similarity of the onion-like inclusion that, if ϵ_{eff} is the effective permittivity of the inclusion as a whole, then ϵ_{eff} is also the effective permittivity of the inclusion from which the two outer layers have been removed (Fig. 2). Section II B introduces the *coating function* $c(\epsilon_2, \epsilon_1)$, which gives the effective permittivity of a spherical inclusion whose core has the permittivity ϵ_2 and that is coated by a spherical layer with the permittivity ϵ_1. Because adding two extra coatings on the self-similar sphere does not affect the effective permittivity, the effective permittivity satisfies a fixed-point condition $\epsilon_{\mathrm{eff}} = c(c(\epsilon_{\mathrm{eff}}, \epsilon_2), \epsilon_1)$. In Sec. III A, the equation that results from the fixed-point condition provides an analytic expression for the effective permittivity ϵ_{eff}.

The coating function $c(\epsilon_2, \epsilon_1)$ concisely encapsulates results that are provided by the theory of core-shell structures, which has been richly studied [8,23,24]. Section II A revisits the theory of core–shells to derive the coating function by using a homogenization principle. Section II B uses the coating function in an inside-out approach that derives an
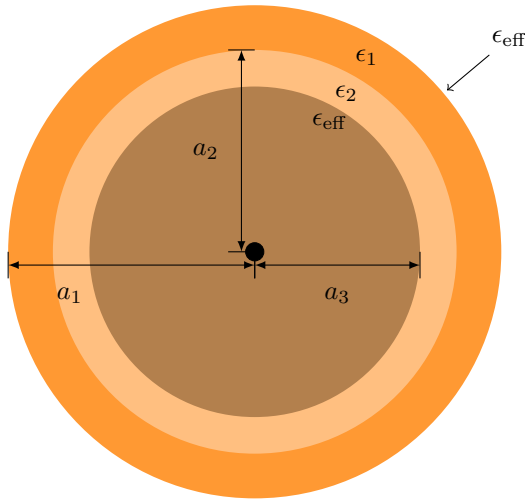
FIG. 2. Analysis of intact self-similar inclusion. If we have guessed the effective permittivity ϵ_{eff} right, coating a homogeneous inclusion of $\epsilon = \epsilon_{\mathrm{eff}}$ with a layer doublet of ϵ_1 and ϵ_2 leaves the effective permittivity of the coated inclusion unchanged. This gives a condition from which ϵ_{eff} can be calculated.

expression for the effective permittivity of a multilayered sphere. This incremental method of *internal homogenization* [23–25] has been found to have great parsimony because it avoids explicitly using a cascade of propagation matrices. Compared with the homogenization approach, the method of propagation matrices is arguably less intuitive, but it relies less on physical insight and therefore generalizes more readily [26,27].

This article chooses to treat the two branches of Eq. (3) without dismissing one of the branches *a priori*. When two separate branches ϵ_α and ϵ_β exist and have different absolute values, we refer to ϵ_α as the *primary* branch and ϵ_β as the *secondary* branch when $|\epsilon_\alpha| < |\epsilon_\beta|$. Although Sec. IV A presents an argument against ϵ_β in an intact inclusion, the same section shows that ϵ_β has relevance when the inclusion is punctured.

Regardless of the physical relevance of the secondary branch ϵ_β, we gain mathematical insight by formally treating ϵ_β as if it had an equal standing with ϵ_α. Section III D establishes a duality between the effective permittivities ϵ_α and ϵ_β and the ordinary layer permittivities ϵ_1 and ϵ_2. Dualities that transpose two intrinsic permittivities are known in the literature [28–30]. However, we present here a duality that interchanges a pair of intrinsic permittivities with a pair of effective permittivities.

This article discusses both the intact self-similar inclusion and the punctured inclusion. Although self-similarity is broken in a punctured inclusion, the deviation from self-similarity diminishes when the core that intervenes the self-similar pattern of alternating layers is made smaller. In Sec. III B, the branches ϵ_α and ϵ_β of the intact inclusion allow us to write the effective permittivity ϵ_{eff} of a punctured inclusion in a concise form that generalizes an existing result.

The final part of the article discusses the implications of the layer implementation on the theory of radially anisotropic spheres. Sections IV A–IV B show that the effective permittiv-
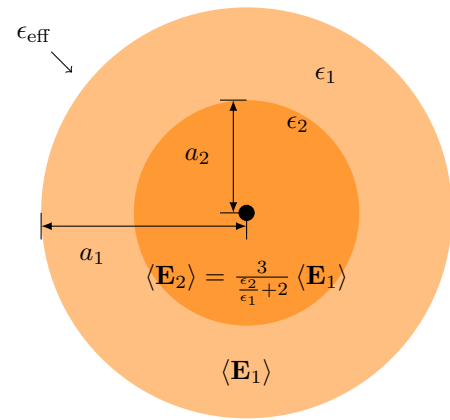

FIG. 3. Core–shell. To homogenize the inclusion, it suffices to find the volume-averaged fields.

ity ϵ_{eff} of a punctured inclusion smoothly transitions between ϵ_α and ϵ_β when the core permittivity ϵ_{c} is adjusted gradually. The sections conceptually discuss possible applications of the phenomenon.

A particularly paradoxical implication of the two-branched indeterminacy of the radially anisotropic sphere and the contrasting determinacy of the punctured sphere is that there are small inclusions that can resist cloaking and remain visible even when a radially anisotropic cloak is applied. Section IV B discusses the paradox and its explanation.

II. PRELIMINARIES

A. Core–shell

Let us first consider a core-shell inclusion that consists of a spherical, homogeneous core with a permittivity ϵ_2 and a radius a_2 coated with a spherical, homogeneous shell with a permittivity ϵ_1 and an outer radius a_1 (Fig. 3).

Because the impinging excitation field $\mathbf{E}^{\mathrm{p}}$ is assumed static and uniform, it follows from the orthogonality of the spherical harmonics that the full solution of the Laplace equation $\nabla^2 \phi = 0$ in the coating reduces to just two terms—the dipole term and the term that gives a uniform field—of which the dipole term vanishes in the core region. When we take the origin of the spherical coordinates at the center of the inclusion, the potentials are

$$\phi_1 = -C_1 \mathbf{E}^{\mathrm{p}} \cdot \mathbf{r} + a_1^3 D_1 \frac{\mathbf{E}^{\mathrm{p}} \cdot \mathbf{r}}{r^3},$$
$$\phi_2 = -C_2 \mathbf{E}^{\mathrm{p}} \cdot \mathbf{r}, \qquad (4)$$

where $U_0 = a_1 E^{\mathrm{p}}$. We apply at the interface the continuity of the potential and the continuity of the normal component of the electric flux density. In terms of potentials, these conditions are given for the spherical surface at $r = a_2$ as

$$\phi_1 = \phi_2,$$
$$\epsilon_1 \frac{\partial \phi_1}{\partial r} = \epsilon_2 \frac{\partial \phi_2}{\partial r}. \qquad (5)$$

When we substitute Eq. (4) and eliminate D_1, we get

$$\frac{C_2}{C_1} = \frac{3}{\frac{\epsilon_2}{\epsilon_1} + 2}. \qquad (6)$$

The equation is just the textbook formula [31, Sec. 3.24] for a homogeneous sphere in a homogeneous background because the essentials of the two problems are the same.

To get the effective permittivity, we need to know the fraction $A = \bar{E}_2/\bar{E}_1$ between the volume-averaged fields $\langle \mathbf{E}_1 \rangle = \bar{E}_1 \mathbf{u}_z$ and $\langle \mathbf{E}_2 \rangle = \bar{E}_2 \mathbf{u}_z$. The fraction A is a simple scalar because the field averages turn out to be parallel. We may parametrize the geometry of the self-similar inclusion by the volume fraction d of the coating, so that

$$d = 1 - \left(\frac{a_2}{a_1}\right)^3.$$

As for the fields, the dipole field may be disregarded in the volume average because the volume integral of a dipole field vanishes over a volume that is bound by two concentric spheres [25, Eq. 20]. That leaves

$$A = \frac{C_2}{C_1} = \frac{3}{\frac{\epsilon_2}{\epsilon_1} + 2}. \qquad (7)$$

The effective permittivity is defined by $\langle \mathbf{D} \rangle = \epsilon_{\text{vac}} \epsilon_{\text{eff}} \langle \mathbf{E} \rangle$, where ϵ_{vac} is the vacuum permittivity and the volume average extends over the entire inclusion, including both the core and the coating. For the chosen parametrization of the core-shell, the definition becomes

$$d\epsilon_1 \bar{E}_1 + (1-d)\epsilon_2 \bar{E}_2 = \epsilon_{\text{eff}}[d\bar{E}_1 + (1-d)\bar{E}_2],$$

which yields a scalar effective permittivity

$$\epsilon_{\text{eff}} = \epsilon_2 + d\frac{\epsilon_1 - \epsilon_2}{A + d(1-A)}$$
$$= \epsilon_2 + d\frac{\epsilon_2 + 2\epsilon_1}{(3-d)\epsilon_1 + d\epsilon_2}(\epsilon_1 - \epsilon_2). \qquad (8)$$

We may check that $\epsilon_{\text{eff}} = \epsilon_2$ when $d = 0$. This corresponds to the special case where the coating does not contribute because its thickness vanishes. Also, we may check that $\epsilon_{\text{eff}} = \epsilon_2$ when $\epsilon_1 = \epsilon_2$. This corresponds to the special case where the coating does not contribute because its material matches that of the core. We may also check that if $\epsilon_1 \neq \epsilon_2$ the contribution of the coating increases together with the volume fraction d of the coating. This too coincides with the expectation.

A different parametrization has also been used in the literature [24,32]. When the volume fraction of the core $g = 1 - d$ is used in Eq. (8) instead of the volume fraction d of the coating, the equation takes the form

$$\epsilon_{\text{eff}} = \epsilon_1 + 3g\epsilon_1 \frac{\epsilon_2 - \epsilon_1}{(\epsilon_2 + 2\epsilon_1) - g(\epsilon_2 - \epsilon_1)}, \qquad (9)$$

which is exactly the form of the Maxwell-Garnett equation in the theory of electromagnetic mixing formulas. The Maxwell-Garnett equation is a mean-field approximation for the effective permittivity of a random dielectric mixture [22, Sec. 3.1]. However, in the particular case of a core-shell, the mean-field approach does not involve an approximation and the result applies exactly.

B. Multilayered sphere

To accommodate multiple layers of coating in the theory, we may repeat the homogenization process of Sec. II A multiple times, starting from the coating that is directly on the core

and proceeding outward. For a convenience of notation, we introduce the *coating function*, defined by

$$c_d(\epsilon_2, \epsilon_1) = \epsilon_2 + d\frac{\epsilon_2 + 2\epsilon_1}{(3-d)\epsilon_1 + d\epsilon_2}(\epsilon_1 - \epsilon_2), \qquad (10)$$

so that, for a core-shell of a core ϵ_2 and a coating ϵ_1, the effective permittivity is $\epsilon_{\text{eff}} = c_d(\epsilon_2, \epsilon_1)$, by Eq. (8). Let us consider a spherical, multilayered inclusion that has the permittivities $\epsilon_1, \epsilon_2, \ldots, \epsilon_N$ proceeding from the outmost layer toward the core. Homogenizing from the core outward, we find that the effective permittivity is

$$\epsilon_{\text{eff}} = c_{d_1}\big(c_{d_2}\big(\ldots \big(c_{d_{N-1}}(\epsilon_N, \epsilon_{n-1}), \ldots\big), \epsilon_2\big), \epsilon_1\big), \qquad (11)$$

where the self-similarity is not yet assumed, so that the volume fractions

$$d_n = 1 - \left(\frac{a_{n+1}}{a_n}\right)^3$$

may take separate values.

III. SELF-SIMILARITY

A. Intact inclusion

The multilayered sphere can have any positive values of the parameters d_n and any complex permittivities ϵ_n. However, the self-similar sphere is a special case where the parameters $d_n = d$ are kept fixed between layers and where the permittivities ϵ_n follow a repeating pattern. For simplicity, we take this pattern to be the pattern of Fig. 1, so that the permittivity alternates between ϵ_1 and ϵ_2. By self-similarity,

$$\epsilon_{\text{eff}} = c_d(c_d(\epsilon_{\text{eff}}, \epsilon_2), \epsilon_1), \qquad (12)$$

so that ϵ_{eff} is the fixed point of the function $c_d(c_d(\cdot, \epsilon_2), \epsilon_1)$.

We now proceed to find the fixed point. It is possible to directly solve the equation that results when Eqs. (10) and (12) are combined. However, it is easier to proceed by first effecting a suitable limit. Because the goal is to implement the radially anisotropic sphere and because the self-similar sphere becomes the analog of the radially anisotropic sphere in the limit $d \to 0^+$, we assume d to be sufficiently small so that higher-order terms of d may be omitted. When the assumption of a thin layer is made, we denote the volume fraction d of the coating by the Greek letter δ. The approximation $\delta^2 = 0$ is assumed implicitly throughout the article. Likewise, γ is introduced in place of the volume fraction g of the core when the fraction is close to unity.

When we linearize Eq. (10), the result is

$$c_\delta(\epsilon_2, \epsilon_1) = \epsilon_2 + \delta\frac{\epsilon_2 + 2\epsilon_1}{3\epsilon_1}(\epsilon_1 - \epsilon_2). \qquad (13)$$

Therefore

$$c_\delta(c_\delta(\epsilon_{\text{eff}}, \epsilon_2), \epsilon_1) = \epsilon_{\text{eff}} + \delta\frac{\epsilon_{\text{eff}} + 2\epsilon_2}{3\epsilon_2}(\epsilon_2 - \epsilon_{\text{eff}})$$
$$+ \delta\frac{\epsilon_{\text{eff}} + 2\epsilon_1}{3\epsilon_1}(\epsilon_1 - \epsilon_{\text{eff}}). \qquad (14)$$

Now Eq. (12) reduces to the quadratic equation

$$\epsilon_{\text{eff}}^2 + \frac{2\epsilon_1\epsilon_2}{\epsilon_1 + \epsilon_2}\epsilon_{\text{eff}} - 2\epsilon_1\epsilon_2 = 0, \qquad (15)$$
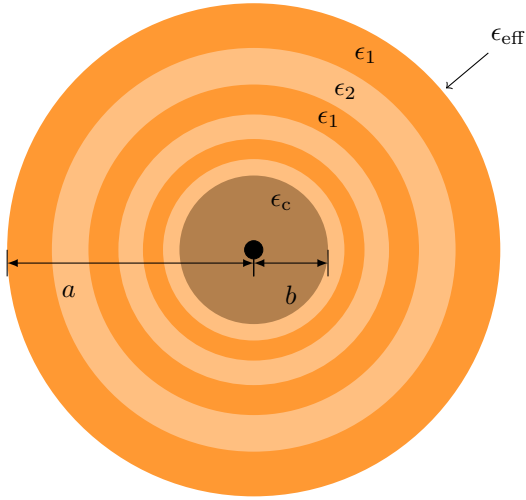
FIG. 4. Punctured inclusion. The self-similarity of the punctured inclusion is only approximate because the pattern of alternating layers is interrupted near the center. Unlike the intact inclusion, the punctured inclusion has a unique effective permittivity ϵ_{eff}, without indeterminacy.

the solution

$$\epsilon_{\text{eff}} = \frac{\epsilon_1 \epsilon_2}{\epsilon_1 + \epsilon_2}\left(\pm\sqrt{1 + 2\frac{(\epsilon_1 + \epsilon_2)^2}{\epsilon_1 \epsilon_2}} - 1\right) \quad (16)$$

of which gives the effective permittivity of the self-similar sphere. The expression is, in general, two-valued because of the two branches of the square root. The present derivation therefore allows two solutions for the effective permittivity and does not fix the electric potential inside the inclusion uniquely.

We may test Eq. (16) by comparing it with the expressions that the literature gives for the radially anisotropic sphere. The capacitor equations (2) transform Eq. (16) into Eq. (3), which is the expression that is already known in the literature [4, Eq. 15].

B. Punctured inclusion

The result (16) in Sec. III A manifests indeterminacy because the quadratic equation from which the result was derived has two solutions. However, because the coating function has a unique value for a given triplet $\delta, \epsilon_1, \epsilon_2$ of arguments, we can use the function to construct a unique solution. In this approach, we first choose an arbitrary value ϵ_c for a finite-size core and add an even number N layers of coating, so that the permittivity again alternates between ϵ_1 and ϵ_2, starting with ϵ_1 at the outmost layer (Fig. 4). A finite inclusion is not strictly self-similar, but if δ is fixed between layers, the finite inclusion approaches the self-similar inclusion when the number N of the coatings increases.

The effective permittivity of the finite inclusion is

$$\epsilon_{\text{eff},n} = \overbrace{c_\delta(c_\delta(\dots(c_\delta(\epsilon_c, \epsilon_2),\dots), \epsilon_2), \epsilon_1)}^{n}. \quad (17)$$

If the sequence $\epsilon_{\text{eff},n}$ converges to a value, it follows that the limit

$$\epsilon_{\text{eff}} = \lim_{n\to\infty} \epsilon_{\text{eff},n}$$

must be a fixed point of $c_\delta(c_\delta(\cdot, \epsilon_2), \epsilon_1)$ and that it must thus satisfy Eq. (12). Therefore, if the sequence converges, it converges to Eq. (16). Also, because the solution is given by a cascade of single-valued functions c_δ and because the only parameter that is chosen arbitrarily is the core permittivity ϵ_c, the sequence must converge in such a manner that the relevant branch of the square root in Eq. (16) is uniquely determined by the choice of the core permittivity ϵ_c.

To see when the sequence (17) converges and to find the limit of the sequence, we assume that the layers are sufficiently thin and numerous to be treated as if they constituted a continuum. When we use this assumption to justify the substitution

$$c_\delta(c_\delta(\epsilon, \epsilon_2), \epsilon_1) - \epsilon = \frac{\Delta\epsilon}{\frac{1}{2}\Delta n} \to \frac{d\epsilon}{d(\frac{1}{2}n)}.$$

The difference equation (14) then transforms into the differential equation

$$\frac{d\epsilon}{d(\frac{1}{2}n)} = \delta\frac{\epsilon + 2\epsilon_2}{3\epsilon_2}(\epsilon_2 - \epsilon) + \delta\frac{\epsilon + 2\epsilon_1}{3\epsilon_1}(\epsilon_1 - \epsilon). \quad (18)$$

Here ϵ stands for the effective permittivity that is accumulated when n layers are added on the core. We denote by ϵ_α and ϵ_β the two solutions of Eq. (15), and only permit $\epsilon_\alpha = \epsilon_\beta$ in the degenerate case where Eq. (15) has a double root. Then Eq. (18) becomes

$$\frac{d\epsilon}{dn} = -\delta\frac{1}{3\epsilon_\parallel}(\epsilon - \epsilon_\alpha)(\epsilon - \epsilon_\beta), \quad (19)$$

where $\epsilon_\parallel$ is defined by the capacitor equation (2). The solution for the first-order differential equation is

$$\epsilon(n) = \epsilon_\beta + \frac{\epsilon_\alpha - \epsilon_\beta}{1 - \frac{\epsilon_c - \epsilon_\alpha}{\epsilon_c - \epsilon_\beta}\exp\left(-\frac{(\epsilon_\alpha - \epsilon_\beta)n\delta}{3\epsilon_\parallel}\right)}, \quad (20)$$

where the factor $(\epsilon_c - \epsilon_\alpha)/(\epsilon_c - \epsilon_\beta)$ in the denominator ensures that $\epsilon = \epsilon_c$ when $n = 0$. If we let b stand for the radius of the core, the number n of the accumulated layers is related to the distance r from the center of the inclusion by

$$n = \frac{3}{\delta}\ln\left(\frac{r}{b}\right). \quad (21)$$

This result, together with the difference

$$\epsilon_\alpha - \epsilon_\beta = \epsilon_\parallel \sqrt[(\alpha)]{1 + 2\frac{(\epsilon_1 + \epsilon_2)^2}{\epsilon_1 \epsilon_2}} \equiv \epsilon_\parallel \sqrt[(\alpha)]{\cdot}$$

between the two solutions to Eq. (16) simplifies the exponential in Eq. (20) to

$$\exp\left(-\frac{(\epsilon_\alpha - \epsilon_\beta)n\delta}{3\epsilon_\parallel}\right) = \left(\frac{b}{r}\right)^{\sqrt[(\alpha)]{\cdot}},$$

where the notation $\sqrt[(\alpha)]{\cdot}$ refers to the branch of the square root in Eq. (16) that gives ϵ_α as the effective permittivity. Finally,

we can set r equal to the outer radius a of the entire inclusion to get

$$\epsilon_{\text{eff}} = \epsilon_\beta + \frac{\epsilon_\alpha - \epsilon_\beta}{1 - \frac{\epsilon_c - \epsilon_\alpha}{\epsilon_c - \epsilon_\beta}\left(\frac{b}{a}\right)^{(\alpha)\sqrt{\cdot}}}, \qquad (22)$$

or the alternative form

$$\epsilon_{\text{eff}} = \frac{\epsilon_\parallel}{2}\left({}^{(\alpha)}\!\sqrt{\cdot}\left(\frac{1 + \frac{\epsilon_c - \epsilon_\alpha}{\epsilon_c - \epsilon_\beta}\left(\frac{b}{a}\right)^{(\alpha)\sqrt{\cdot}}}{1 - \frac{\epsilon_c - \epsilon_\alpha}{\epsilon_c - \epsilon_\beta}\left(\frac{b}{a}\right)^{(\alpha)\sqrt{\cdot}}} \right) - 1 \right),$$

which generalizes an earlier result [4, Eq. 23] that assumes a perfectly electrically conducting (PEC) core. As one might expect, ϵ_{eff} is determined by the intrinsic material parameters and the *core-shell ratio* b/a.

The sequence (17) converges to the value given by Eq. (22) in the limit $b/a \to 0$ when the limit exists. It follows from the properties of the exponent function that the limit exists whenever the square root ${}^{(\alpha)}\!\sqrt{\cdot}$ has a nonvanishing real part. If the square root $\sqrt{\cdot}$ has a nonvanishing real part, we can choose the labels α and β so that the real part of ${}^{(\alpha)}\!\sqrt{\cdot}$ is positive. This is because the order of labels for the permittivities ϵ_α and ϵ_β have so far been arbitrary. With this convention, ${}^{(\alpha)}\!\sqrt{\cdot}$ is just the canonical square root. It can be seen from Eq. (22) that ϵ_α now refers to the stable fixed point and ϵ_β to the unstable one and that both of these cannot be stable at the same time. We will hereafter adopt the convention that ϵ_α always stands for the stable fixed point when one exists.

The solution (22) oscillates indefinitely when the discriminant under the square root ${}^{(\alpha)}\!\sqrt{\cdot}$ is real and negative. The condition $\text{Im}\{\cdot\} = 0$ is met when $\epsilon_1/|\epsilon_1| = \pm\epsilon_2/|\epsilon_2|$ or $|\epsilon_1| = |\epsilon_2|$. The last alternative is only compatible with $\text{Re}\{\cdot\} > 0$ and therefore only yields convergent solutions. Indefinite oscillations then require that the complex permittivities ϵ_1 and ϵ_2 have parallel or opposite direction factors. The necessary and sufficient condition turns out to be that $\epsilon_2/\epsilon_1 \in \mathbb{R} \setminus \{0\}$ and

$$\frac{\epsilon_2}{\epsilon_1} < -2 \quad \text{or} \quad \frac{\epsilon_1}{\epsilon_2} < -2. \qquad (23)$$

It may be noted that this condition does not preclude indefinite oscillations of the solution (22) when one of the layer materials is lossy and the other material is active.

Condition (23) may also be stated in terms of the parameters of a radially anisotropic coating. It follows from the capacitor equations (2) that, when the layer permittivities are multiplied by some scalar factor k, so that $\epsilon_1 \to k\epsilon_1$ and $\epsilon_2 \to k\epsilon_2$, the components of the radially anisotropic permittivity get multiplied by the same scalar, i.e., $\epsilon_\parallel \to k\epsilon_\parallel$ and $\epsilon_\perp \to k\epsilon_\perp$. It follows from this that $\epsilon_\perp/\epsilon_\parallel$ is real at the same time with ϵ_2/ϵ_1—barring singularities. It then follows from Eq. (23) that a necessary condition for the indefinite oscillations is $\epsilon_\perp/\epsilon_\parallel < -1/8$, where the fraction must be real. The sufficiency of the condition can be seen by replacing the square root ${}^{(\alpha)}\!\sqrt{\cdot}$ with the one in Eq. (3). In conclusion, condition (23) accords with the literature [4, Sec. 2.4.].

C. Internal field

Let us resume the discussion of the intact inclusion, so that the self-similarity is again exact. The introduction stated that
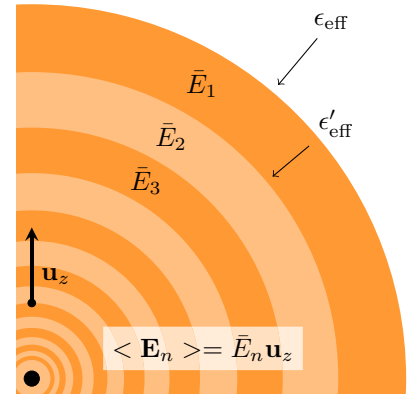

FIG. 5. Average fields of outer layers. The average fields are all oriented along the z axis. The effective permittivity may change infinitesimally from ϵ_{eff} to ϵ'_{eff} when the outmost layer is peeled from the inclusion.

the analogy between the self-similar sphere and the radially anisotropic sphere requires both the external and the internal potentials to coincide. The external potentials coincide because these potentials are determined by the effective permittivities in Eqs. (3) and (16) and because Sec. III A found these to be equivalent. We may now consider the internal potentials, starting with the corresponding fields.

Two different effective permittivities ϵ_{eff} and ϵ'_{eff} are relevant. Of these two, ϵ_{eff} refers to the effective permittivity of the entire inclusions and is, by self-similarity, also to the effective permittivity of every inner sphere that starts with an outer layer of permittivity ϵ_1. Likewise, ϵ'_{eff} refers to the effective permittivity of each inner sphere that starts with an outer layer of permittivity ϵ_2. Although the difference $\epsilon'_{\text{eff}} - \epsilon_{\text{eff}}$ is, by Eq. (13), of order δ and cannot therefore be neglected in general, the derivation (24)–(26) below only features ϵ'_{eff} in the product $\delta\epsilon'_{\text{eff}}$, in which context the two effective permittivities can be regarded as equal.

Let $\langle \mathbf{E} \rangle = \bar{E}\mathbf{u}_z$ be the average field of the entire inclusion, apart from the three outmost layers. The field averages $\bar{E}_1$, $\bar{E}_2$, and $\bar{E}_3$ of the three outmost layers (Fig. 5) are then

$$\bar{E}_3 = \frac{\epsilon_{\text{eff}} + 2\epsilon_1}{3\epsilon_1}\bar{E}, \qquad (24)$$

$$\bar{E}_2 = \frac{\epsilon'_{\text{eff}} + 2\epsilon_2}{3\epsilon_2}(\delta\bar{E}_3 + \gamma\bar{E}), \qquad (25)$$

$$\bar{E}_1 = \frac{\epsilon_{\text{eff}} + 2\epsilon_1}{3\epsilon_1}(\delta\bar{E}_2 + \delta\gamma\bar{E}_3 + \gamma^2\bar{E}), \qquad (26)$$

where again $\gamma = 1 - \delta$. When we substitute Eqs. (24) and (25) into Eq. (26), we get

$$\frac{\bar{E}_1}{\bar{E}_3} = 1 + \delta\left(\frac{\epsilon_{\text{eff}} + 2\epsilon_1}{3\epsilon_1} + \frac{\epsilon_{\text{eff}} + 2\epsilon_2}{3\epsilon_2} - 2\right),$$

where again the terms with δ^2 have been omitted. It follows that

$$\frac{\bar{E}_3}{\bar{E}_1} = 1 - \delta\left(\frac{\epsilon_{\text{eff}} + 2\epsilon_1}{3\epsilon_1} + \frac{\epsilon_{\text{eff}} + 2\epsilon_2}{3\epsilon_2} - 2\right)$$

$$= 1 - \frac{2}{3}\delta\left(\frac{\epsilon_{\text{eff}}}{\epsilon_\parallel} - 1\right).$$
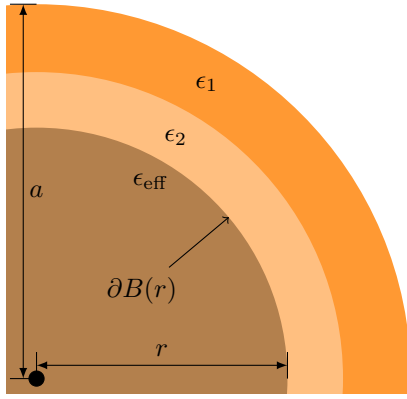
FIG. 6. Partly homogenized self-similar sphere. The potential is affected by the homogenization only inside the homogenized region.

Then, because by self-similarity all such fractions between proximate odd layers are the same, for an odd layer n

$$\frac{\bar{E}_n}{\bar{E}_1} = \left[1 - \frac{2}{3}\delta\left(\frac{\epsilon_{\text{eff}}}{\epsilon_{\parallel}} - 1\right) \right]^{n/2}$$
$$= \exp\left[-\frac{1}{3}\delta\left(\frac{\epsilon_{\text{eff}}}{\epsilon_{\parallel}} - 1\right)n \right]. \qquad (27)$$

For the punctured inclusion, the respective n is given by Eq. (21). However, the indexing, in the present context, starts from the outmost layer and not from a core, as was the case with the punctured inclusion. Therefore, Eq. (21) gets modified into

$$n = \frac{3}{\delta}\ln\left(\frac{a}{r}\right), \qquad (28)$$

which with Eq. (27) and with an analogous derivation for the even layers gives

$$\bar{E}_{\text{odd}}(r) = \bar{E}_1\left(\frac{r}{a}\right)^{\frac{\epsilon_{\text{eff}}}{\epsilon_{\parallel}}-1}, \quad \bar{E}_{\text{even}}(r) = \bar{E}_2\left(\frac{r}{a}\right)^{\frac{\epsilon_{\text{eff}}}{\epsilon_{\parallel}}-1}. \qquad (29)$$

Let us now consider a spherical volume $B(r)$ that is concentric with the inclusion and has its radius r inside the radius a of the inclusion (Fig. 6). When the material is homogenized over $B(r)$ the potential $\phi(r,\theta)$ inside the inclusion remains unaffected at the surface $\partial B(r)$ of the homogenized region and outside it. However, inside $B(r)$ the potential is that of a uniform electric field. If the homogenized region $B(r)$ were chosen to cover the entire inclusion, so that $r = a$, the homogenized potential would be

$$\phi(\mathbf{r})|_{r=a} = -\frac{3}{\epsilon_{\text{eff}} + 2}\mathbf{E}^{\text{p}} \cdot \mathbf{r},$$

at the surface [31, Sec. 3.24.]. It follows from the proportionalities (29) that, for a smaller homogenized region $B(r)$ with $r < a$, a scaling must be introduced. The potential at the surface $\partial B(r)$ of the homogenized region in this case is then

$$\phi(\mathbf{r}) = -\frac{3}{\epsilon_{\text{eff}} + 2}\left(\frac{r}{a}\right)^{\frac{\epsilon_{\text{eff}}}{\epsilon_{\parallel}}-1}\mathbf{E}^{\text{p}} \cdot \mathbf{r}. \qquad (30)$$

But this is also the potential inside the original self-similar inclusion, without the homogenization, because the potential
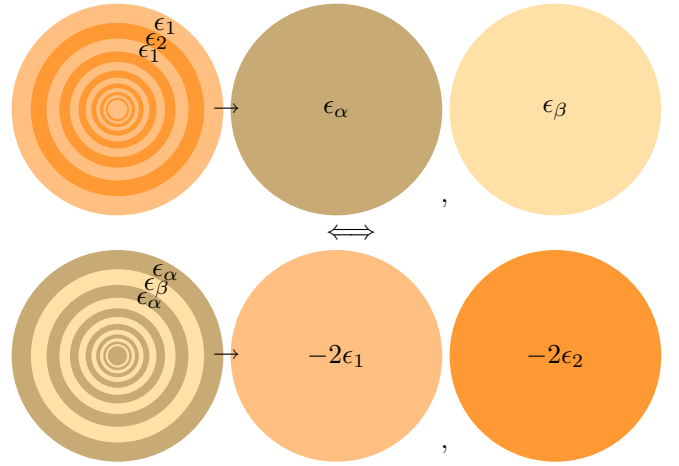

FIG. 7. Duality. The layer permittivities ϵ_1 and ϵ_2 are interchangeable with the effective permittivities ϵ_α and ϵ_β, apart from an extra factor -2.

at the surface $\partial B(r)$ remains unchanged by the homogenization. The result in Eq. (30) gives the same potential that the literature gives for the radially anisotropic sphere [4, Eqs. 9,12].

D. Duality

The two pairs of material parameters, ϵ_1, ϵ_2 and $\epsilon_\alpha, \epsilon_\beta$, stand in an almost symmetric relation with one another. An inexact duality exists between the two pairs (Fig. 7). The approximate duality can be shown by a direct substitution. Let ϵ_α and ϵ_β again be the two branches of the effective permittivity and assume that $\epsilon_\alpha \neq \epsilon_\beta$ if two distinct branches exist. By Eq. (16), the condition

$$\epsilon_\alpha = c_\delta(c_\delta(\epsilon_\alpha, \epsilon_2), \epsilon_1),$$
$$\epsilon_\beta = c_\delta(c_\delta(\epsilon_\beta, \epsilon_2), \epsilon_1) \qquad (31)$$

is fulfilled if and only if

$$\epsilon_\alpha, \epsilon_\beta = \frac{\epsilon_1\epsilon_2}{\epsilon_1 + \epsilon_2}\left(\sqrt[{(\alpha,\beta)}]{1 + 2\frac{(\epsilon_1 + \epsilon_2)^2}{\epsilon_1\epsilon_2}} - 1 \right). \qquad (32)$$

By direct substitution, it can be checked that, with ϵ_α and ϵ_β given by Eq. (32), the equations

$$-2\epsilon_1 = c_\delta(c_\delta(-2\epsilon_1, \epsilon_\beta), \epsilon_\alpha),$$
$$-2\epsilon_2 = c_\delta(c_\delta(-2\epsilon_2, \epsilon_\beta), \epsilon_\alpha) \qquad (33)$$

are satisfied. One may repeat the process, starting from Eq. (33) and arriving at Eq. (31). The two pairs of equations, (31) and (33), are therefore equivalent. The result says that the roles of the layer permittivities ϵ_1, ϵ_2 and the effective permittivities $\epsilon_\alpha, \epsilon_\beta$ can be interchanged, apart from a factor -2 which multiplies the novel effective permittivities (Fig. 7).

The duality property becomes useful when we want to find layer permittivities ϵ_1 and ϵ_2 that fix the effective permittivities ϵ_α and ϵ_β at specified values. By Eq. (33), it suffices to find the two fixed points of $c_\delta(c_\delta(\cdot, \epsilon_\beta), \epsilon_\alpha)$ and divide by -2.

Therefore,

$$\epsilon_{1,2} = -\frac{1}{2}\frac{\epsilon_\alpha\epsilon_\beta}{\epsilon_\alpha+\epsilon_\beta}\left({}^{(1,2)}\sqrt{1+2\frac{(\epsilon_\alpha+\epsilon_\beta)^2}{\epsilon_\alpha\epsilon_\beta}}-1\right) \qquad (34)$$

gives the desired layer permittivities.

IV. IMPLICATIONS

A. Branch hopping

Section III B demonstrated—in agreement with foregoing research of radial anisotropy [4, Sec. 2.4]—that the ambiguity in Eq. (16) for the effective permittivity of the intact self-similar inclusion may be removed by puncturing the inclusion with a spherical homogeneous core. The effective permittivity ϵ_{eff} of the punctured inclusion is unique. It also converges to a limit when $b/a \rightarrow 0$, unless condition (23) for the indefinite oscillations is fulfilled. If the effective permittivity does approach a limit, the limit is $\epsilon_{\text{eff}} \rightarrow \epsilon_\alpha$ apart from the unusual situation where the core permittivity is given by $\epsilon_c = \epsilon_\beta$. When the core permittivity ϵ_c takes this special value, Eq. (19) implies that the effective permittivity is unaffected by the layers that are added on the core and is therefore independent of the core-shell ratio b/a. In this case, $\epsilon_{\text{eff}} = \epsilon_\beta$ holds even when the core is arbitrarily small compared with the entire inclusion.

It follows that the intact inclusion can be implemented with a punctured inclusion in two essentially different ways, $\epsilon_c \neq \epsilon_\beta$ or $\epsilon_c = \epsilon_\beta$, when the core of the punctured inclusion is infinitesimally small, and that the electric response of the inclusion depends on the chosen implementation. What makes this conclusion surprising is that the more special implementation, $\epsilon_c = \epsilon_\beta$, corresponds to an intact inclusion that withholds an infinite energy in its internal field. To show that the energy of the internal field really does become infinite when the secondary branch ϵ_β of the effective permittivity ϵ_{eff} is chosen, we can find the energy inside a given infinitesimal layer of the inclusion and then aggregate the energy over the layers.

Some preliminary results are needed. Let us denote $f(r,\theta) \sim g(r,\theta)$ when a non-negative real number $A(\theta)$ exist for each θ so that $f(r,\theta) = A(\theta)g(r,\theta)$. The coefficient of proportionality, $A(\theta)$, can vanish for a given θ but it must be finite. Because the proportionality is defined more loosely than what is customary, the relation $f(r,\theta) \sim g(r,\theta)$ is reflexive and transitive but not symmetric.

The dipole field $\mathbf{E}_d(\mathbf{r})$ observed at $\mathbf{r}$ and generated by the part of the self-similar inclusion that falls inside the radius r has the proportionality

$$\|\mathbf{E}_d(\mathbf{r})\| \sim \left\|\frac{3(\mathbf{p}(r)\cdot\mathbf{u}_r)\mathbf{u}_r - \mathbf{p}(r)}{r^3}\right\| \sim \frac{|p(r)|}{r^3} \sim |\bar{E}(r)|, \quad (35)$$

where $p(r)$ is the dipole moment inside the radius r. The last proportionality follows from self-similarity because, by self-similarity, the polarizability of any subset of the inclusion that is spherically symmetric about the origin must be the same when scaled by the volume inside its radius r.

The field in each layer is a combination of a uniform field and a dipole field, so that in a given layer at distance r from the center the field is $\mathbf{E}(\mathbf{r}) = \bar{E}(r)\mathbf{u}_z + \mathbf{E}_d(\mathbf{r})$. The square of

the field is

$$\|\mathbf{E}(\mathbf{r})\|^2 = |\bar{E}(r)|^2 + \|\mathbf{E}_d(\mathbf{r})\|^2$$
$$+ 2|\bar{E}(r)|\|\mathbf{E}_d(\mathbf{r})\|\cos\left[\angle(\mathbf{E}_d,\mathbf{u}_z)\right],$$

which with Eq. (35) gives $\|\mathbf{E}(\mathbf{r})\| \sim |\bar{E}(r)|$.

Next, we may calculate the energy. The energy density in a homogeneous medium is [31, Sec. 2.8.]

$$u = \tfrac{1}{2}\epsilon_{\text{vac}}\epsilon\|\mathbf{E}\|^2,$$

where ϵ_{vac} is the vacuum permittivity. The absolute value of the energy is given by

$$\left|\int_\mathcal{V} u\,dV\right| = \left|\int_\mathcal{V}\frac{\epsilon_{\text{vac}}\epsilon_1}{2}\mathbf{E}_{\text{odd}}^2\frac{dV}{2} + \int_\mathcal{V}\frac{\epsilon_{\text{vac}}\epsilon_2}{2}\mathbf{E}_{\text{even}}^2\frac{dV}{2}\right|$$

$$\sim \int_\mathcal{V}|\bar{E}(r)|^2 dV \sim \int_\mathcal{V}\left|\left(\frac{r}{a}\right)^{\frac{\epsilon_{\text{eff}}}{\epsilon_\|}-1}\right|^2 dV$$

$$\sim \int_0^a\left|\left(\frac{r}{a}\right)^{\frac{\epsilon_{\text{eff}}}{\epsilon_\|}}\right|^2 dr = \int_0^a\left(\frac{r}{a}\right)^{2\text{Re}\{\frac{\epsilon_{\text{eff}}}{\epsilon_\|}\}} dr.$$

The proportionality, as it is defined in this section, does not preclude a situation where the two energy integrals over the two types of layers diverge while their integrands cancel out one another so that sum of the integrals vanishes. However, let us assume that the energy does not vanish in this way. In this case, it follows that the energy remains finite if and only if $\text{Re}\{\epsilon_{\text{eff}}/\epsilon_\|\} > -1/2$, i.e., if and only if the primary branch ϵ_α of the effective permittivity ϵ_{eff} exists and is chosen.

The energy condition is commonly used to remove indeterminacy, following Meixner's (1972) treatment of singular fields at edges [33]. Even when the energy condition precludes intact inclusions that manifest the secondary branch ϵ_β of the effective permittivity, the secondary branch can be implemented with a punctured inclusion. This conclusion shows that even the solutions that the energy condition would exclude can have physical significance. The punctured inclusion with $\epsilon_c = \epsilon_\beta$, however, does not violate the energy condition in general because the punctured inclusion is obtained from the intact inclusion by homogenizing a small spherical region around the center and this process does not generally preserve energy.

To establish the physical significance of the secondary branch ϵ_β more firmly, we show that the effective permittivity ϵ_{eff} of a punctured inclusion continuously transitions from ϵ_α to ϵ_β when the core permittivity ϵ_c varies around ϵ_β (Fig. 8). Let us employ Eq. (34) to find the layer permittivities ϵ_1 and ϵ_2 that place the stable and unstable fixed points at suited locations in the complex plane. We place the unstable fixed point $\epsilon_\beta = 1$ at unity, so that the inclusion becomes transparent under favorable circumstances. Also, we place the other fixed point $\epsilon_\alpha = 0.1$ inside the unit circle to make it stable. The real part of the core permittivity ϵ_c is taken to coincide with ϵ_β, so that only the imaginary part $\text{Im}\{\epsilon_c\}$ varies. In this numerical example, the effective permittivity ϵ_{eff} of the punctured inclusion is calculated by using Eq. (22). The transition of ϵ_{eff} between the branches ϵ_α and ϵ_β is smooth, in the mathematical sense, but becomes increasingly abrupt
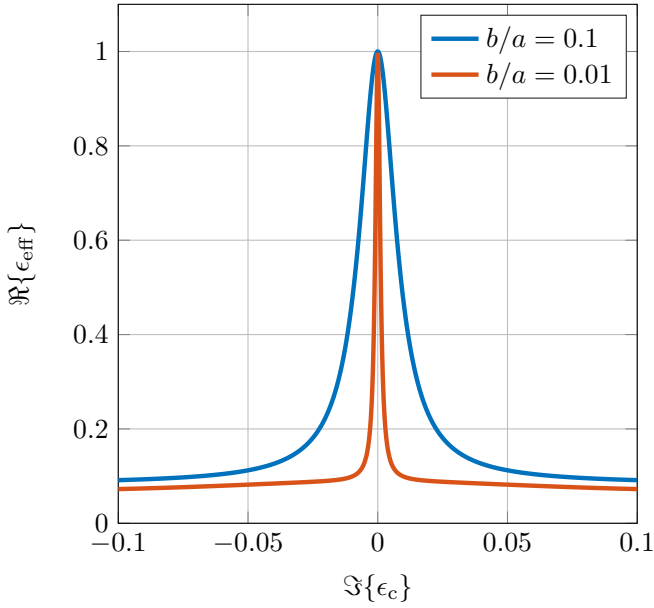
FIG. 8. Branch hop from scattering to transparency. The stable and unstable fixed points are $\epsilon_\alpha = 0.1$ and $\epsilon_\beta = 1$. The core permittivity is $\epsilon_c = 1 + \text{Im}\{\epsilon_c\}j$. Transparency results for a narrow range of the core permittivity. The transition between the fixed points becomes sharper when the core-shell ratio diminishes.
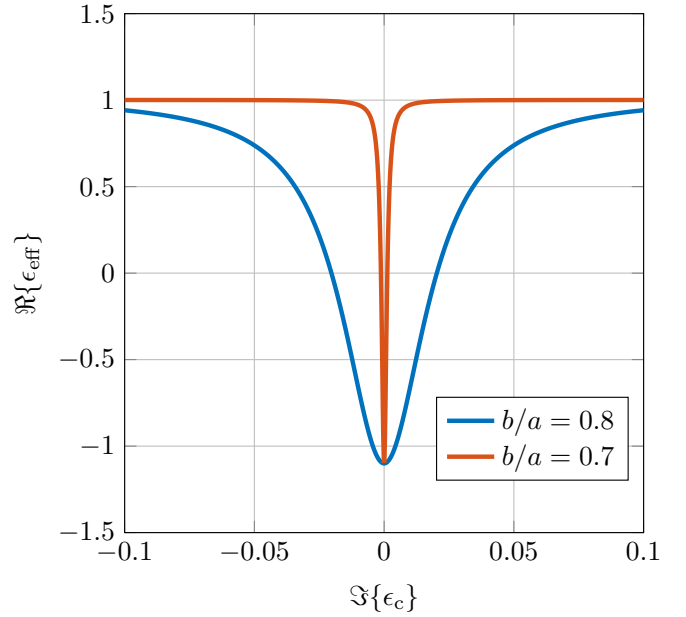

FIG. 9. Emergent scattering from a transparent, cloaking inclusion. The stable and unstable fixed points are $\epsilon_\alpha = 1$ and $\epsilon_\beta = -1.1$. The core permittivity is $\epsilon_c = -1.1 + \text{Im}\{\epsilon_c\}j$. The transition between the fixed points is abrupt even when the core constitutes a substantial part of the inclusion's volume.

when the core-shell ratio b/a diminishes. We refer to the transition between the branches as *branch hopping*.

Because the inclusion tends to normally scatter an incident electric field and because the inclusion abruptly becomes transparent when $\text{Im}\{\epsilon_c\} = 0$, the inclusion can theoretically serve as an optical bandpass filter of a Q factor that can be made as high as needed by diminishing the core-shell ratio b/a sufficiently. If we assume the idealization that the layer permittivities ϵ_1 and ϵ_2 are nondispersive so that the angular frequency ω affects only the core permittivity ϵ_c of the inclusion and if we further assume that the ω dependence is linear and pure imaginary, so that $\epsilon_c = \epsilon_\beta + j\omega\Delta\epsilon_c$, the dispersion curve $\epsilon_{\text{eff}}(\omega)$ of the effective permittivity of the punctured inclusion follows the trajectory shown in Fig. 8, apart from the scaling of the x axis.

B. Emergent scattering

A special case of branch hopping is a response from an inclusion that would normally cloak its core but fails to achieve the cloaking effect because the carefully tailored core activates the secondary branch of the inclusion's effective permittivity, making the inclusion visible. It might be somewhat unexpected that the core, regardless of its possibly infinitesimal size, should be able to enact this transformation because the cloaking effect of the inclusion tends to strongly deviate electric-field lines from its center so that only a very small electric field is incident on the core initially [4, Fig. 4]. However, the literature presents cases where it is precisely the small scale of a geometric feature that enhances scattering or absorption by more strongly localizing electric interactions. In particular, enhanced scattering and absorption have been

associated with a high curvature in the corner of a slightly blunted wedge [34]. Analogously, here the high curvature of the surface of a small core of a punctured self-similar inclusion has a localizing effect that enhances scattering to an extent that overwhelms the cloaking effect.

To demonstrate emergent scattering from a cloaked core, we would like to interchange the roles of the stable and unstable fixed points ϵ_α and ϵ_β in Sec. IV A so that $\epsilon_\alpha = 1$ is the primary branch and the inclusion transitions from transparency to scattering. However, there is no way to interchange the roles of ϵ_α and ϵ_β without moving one or both of them because the priority of a given branch is determined by its location in the complex plane in relation to the other branch.

More specifically, we will now show that $|\epsilon_\alpha| < |\epsilon_\beta|$ when a stable fixed point exists. Let us denote $\sqrt[(\alpha)]{\cdot} = a + bi$ and $\sqrt[(\beta)]{\cdot} = -a - bi$, where $\sqrt[(\alpha)]{\cdot}$ is the canonical square root, so that $a \geqslant 0$. Stability requires that, more strictly, $a > 0$. By Eq. (16), we now have

$$|\epsilon_\alpha| = C|(a-1)+bi| = C\sqrt{(a-1)^2 + b^2},$$

$$|\epsilon_\beta| = C|(a+1)+bi| = C\sqrt{(a+1)^2 + b^2},$$

where $C = |\epsilon_1\epsilon_2/(\epsilon_1 + \epsilon_2)|$. The conclusion follows from $(a-1)^2 < (a+1)^2$.

The requirement that the inclusion must be transparent in the steady state fixes the location $\epsilon_\alpha = 1$ of the primary branch. It follows that the other branch ϵ_β must be placed outside the complex unit circle. We place it at $\epsilon_\beta = -1.1$, in conformity with [4, Fig. 4]. For a numerical example, we calculate the layer permittivities by Eq. (34) and then the effective permittivity of the punctured inclusion by Eq. (22).

As in Sec. IV A, we allow the imaginary part Im{ϵ_c} of the core permittivity to vary while keeping all other parameters fixed. What results is a smooth transition from transparency to scattering, with a more abrupt transition when the core-shell ratio is smaller (Fig. 9).

Because the inclusion does not normally create a perturbation field and because it creates one in the special circumstance that has the imaginary part of the core permittivity vanish, Im{ϵ_c} = 0, the inclusion can theoretically serve as an optical bandstop filter. Also, the Q factor of the bandstop filter can theoretically be made as high as needed by sufficiently diminishing the core-shell ratio b/a. With the chosen material parameters, the Q factor will increase steeply when the core diminishes.

V. CONCLUSION

In this article, we derived the electrostatic response of a spherical self-similar inclusion and showed that the inclusion precisely implements a radially anisotropic sphere. In particular, we showed that both the perturbation field and the internal field of the self-similar sphere match the corresponding fields of a radially anisotropic sphere.

In Sec. III A, we used homogenization as the primary tool to show that the perturbation fields of the self-similar sphere and the radially anisotropic sphere match. We adopted a perturbation approach and required that an infinitesimal double-layer coating should not affect the effective permittivity of a self-similar inclusion even infinitesimally. From this condition, we derived the effective permittivity of the self-similar inclusion. In Sec. III B, we continued to use homogenization to show that the internal field of the self-similar sphere matches the internal field of the radially anisotropic sphere.

Section III D showed that the effective permittivities of a self-similar inclusion are interchangeable with the layer permittivities of the inclusion. Whether the duality between the two pairs of permittivities is accidental or reflects a deeper underlying principle, remains an open question. In any case, we found the duality useful when we tuned the material parameters of the inclusion to meet given specifications in Secs. IV A and IV B.

Both the radially anisotropic sphere and the self-similar sphere have an indeterminacy of material parameters in the center but the character of the indeterminacy varies between the inclusions. The self-similar inclusion has the indeterminacy because the alternating pattern of its layers continues indefinitely toward the center. In contrast, the radially anisotropic inclusion has the indeterminacy because the radial unit vector has no unique orientation in the center. Regardless, the analogy between the self-similar inclusion and the radially anisotropic inclusion holds even in the way that their respective indeterminacies manifest themselves. In fact, Sec. III A showed that the self-similar sphere can generally be homogenized into two distinct homogeneous spheres, with different material parameters. The conclusion coincides with the two-valuedness of the homogenized permittivity for the radially anisotropic sphere. Furthermore, Sec. III B showed that the indeterminacy of the self-similar inclusion can be removed by puncturing, i.e., replacing the material inside a small spherical region around the center by a homogeneous

material. The conclusion generalizes what has been known about the puncturing of radially anisotropic spheres.

This article has attempted to find the physical significance for both branches of the two-valued homogenized permittivity of the self-similar inclusion. Even when Sec. IV A showed that the secondary branch violates the condition that the energy will have to remain finite inside the inclusion, the energy condition is no longer necessarily violated after puncturing. Therefore, the secondary branch can be implemented with a punctured inclusion. Section IV A further showed by a numerical example that the transition between the two branches is continuous and that the continuous transition between the branches can theoretically be used to implement a bandpass filter.

Because the two branches result from the indeterminacy at the center of the inclusion, one could expect that the significance of the indeterminacy diminishes when the layered coating only permits a small part of the excitation field to impinge the center region, as would be the case when the inclusion is designed to operate as a cloak. However, it turns out that the difference between the two branches can be significant, and cloaking merely affects the precision to which the core must be tuned when puncturing the inclusion. Section IV B showed that especially a very small core must be tuned with a pinpoint precision to make the core overcome the cloaking effect.

To keep the analysis simple, we assumed that the self-similar inclusion only has two types of layers and that the two types of layers are equally thick. However, the assumption does not make the conclusions much less general because an inclusion with more than two types of layers can be reduced into an analog that has two types. Also, layers that are not equally thick can be treated as if they were when the difference in the relative thicknesses is compensated by adjusting the permittivities. The more varied set of layers can be useful when one wants to practically implement a special dispersion profile. But the goal of the article was to establish concepts.

Because the presently introduced method only applies to perfectly spherical geometry, it cannot show whether the branch-hopping effect of Secs. IV A and IV B is sensitive to small perturbations in the spherical geometry. The question of small perturbations is critical when one considers the practical applications of the layered sphere. However, the question can only be answered by a separate analysis.

We use the self-similarity as a tool for solving an electrostatic scattering problem. It could be possible to employ the same method to other problems in electrostatics. Hypothetically, one could use the method to derive approximate solutions for radially anisotropic spheroids and ellipsoids. Exact solutions could be available for two other important special cases of spheroids: the flat circular disk and the infinite circular cylinder. For radially anisotropic spheres, the solution could be made more general by allowing the material to be nonlinear. The more general material could then enable new applications besides the bandpass and bandstop filters that were demonstrated. Specifically, branch-hopping can be used to amplify the nonlinearity of a weakly nonlinear core material so that the effective permittivity of the self-similar inclusion can be controlled by the field intensity and the self-similar inclusion functions as an all-optical switch.

Because the method that the article presented is different from the customary, the method can suggest concepts that would otherwise remain elusive. Self-similarity offers a treatment for a familiar scattering problem in electrostatics.

[1] L. Gao, T. H. Fung, K. W. Yu, and C. W. Qiu, Electromagnetic transparency by coated spheres with radial anisotropy, Phys. Rev. E **78**, 046609 (2008).

[2] C.-W. Qiu, A. Novitsky, H. Ma, and S. Qu, Electromagnetic interaction of arbitrary radial-dependent anisotropic spheres and improved invisibility for nonlinear-transformation-based cloaks, Phys. Rev. E **80**, 016604 (2009).

[3] H. Kettunen, H. Wallén, and A. Sihvola, Cloaking and magnifying using radial anisotropy, J. Appl. Phys. **114**, 044110 (2013).

[4] H. Wallén, H. Kettunen, and A. Sihvola, Anomalous absorption, plasmonic resonances, and invisibility of radially anisotropic spheres, Radio Sci. **50**, 18 (2015).

[5] C.-W. Qiu, L. Hu, X. Xu, and Y. Feng, Spherical cloaking with homogeneous isotropic multilayered structures, Phys. Rev. E **79**, 047602 (2009).

[6] F. Mangini, N. Tedeschi, F. Frezza, and A. Sihvola, Homogenization of a multilayer sphere as a radial uniaxial sphere: Features and limits, J. Electromag. Waves Applic. **28**, 916 (2014).

[7] J. Roth and M. Dignam, Scattering and extinction cross sections for a spherical particle coated with an oriented molecular layer, J. Opt. Soc. Am. **63**, 308 (1973).

[8] A. Güttler, Die miesche theorie der beugung durch dielektrische kugeln mit absorbierendem kern und ihre bedeutung für probleme der interstellaren materie und des atmosphärischen aerosols, Ann. Phys. (Berlin, Ger.) **446**, 65 (1952).

[9] K. Schulgasser, Sphere assemblage model for polycrystals and symmetric materials, J. Appl. Phys. **54**, 1380 (1983).

[10] K.-L. Wong and H.-T. Chen, Electromagnetic scattering by a uniaxially anisotropic sphere, IEE Proc. H: Microw. Antenn. Propag. **139**, 314 (1992).

[11] J. C.-E. Sten, DC fields and analytical image solutions for a radially anisotropic spherical conductor, IEEE Trans. Dielectr. Electr. Insul. **2**, 360 (1995).

[12] C.-W. Qiu, L.-W. Li, T.-S. Yeo, and S. Zouhdi, Scattering by rotationally symmetric anisotropic spheres: Potential formulation and parametric studies, Phys. Rev. E **75**, 026609 (2007).

[13] C.-W. Qiu and B. Luk'yanchuk, Peculiarities in light scattering by spherical particles with radial anisotropy, J. Opt. Soc. Am. A **25**, 1623 (2008).

[14] C.-W. Qiu, L. Gao, J. Joannopoulos, and M. Soljačić, Light scattering from anisotropic particles: Propagation, localization, and nonlinearity, Laser Photon. Rev. **4**, 268 (2010).

[15] J. C. de Munck, The potential distribution in a layered anisotropic spheroidal volume conductor, J. Appl. Phys. **64**, 464 (1988).

[16] T. Rimpiläinen, H. Wallén, and A. Sihvola, Radial anisotropy in spheroidal scatterers, IEEE Trans. Antenn. Propag. **63**, 3127 (2015).

[17] T. Rimpiläinen, H. Wallén, H. Kettunen, and A. Sihvola, Electrical response of systropic sphere, IEEE Trans. Antenn. Propag. **60**, 5348 (2012).

[18] T. Rimpiläinen, M. Pitkonen, H. Wallén, H. Kettunen, and A. Sihvola, General systropy in spherical scatterers, IEEE Trans. Antenn. Propag. **62**, 327 (2014).

[19] Y. Huang, Y. Feng, and T. Jiang, Electromagnetic cloaking by layered structure of homogeneous isotropic materials, Opt. Express **15**, 11133 (2007).

[20] Y. Ni, L. Gao, and C.-W. Qiu, Achieving invisibility of homogeneous cylindrically anisotropic cylinders, Plasmonics **5**, 251 (2010).

[21] T. Rimpiläinen, H. Wallén, and A. Sihvola, Polarizability of radially anisotropic elliptic inclusion, J. Appl. Phys. **119**, 014107 (2016).

[22] A. Sihvola, *Electromagnetic Mixing Formulas and Applications* (The Institution of Electrical Engineers, London,1999), p. 284.

[23] Y. Zeng, Q. Wu, and D. Werner, Electrostatic theory for designing lossless negative permittivity metamaterials, Opt. Lett. **35**, 1431 (2010).

[24] U. K. Chettiar and N. Engheta, Internal homogenization: Effective permittivity of a coated sphere, Opt. Express **20**, 22976 (2012).

[25] A. Sihvola and I. Lindell, Polarizability and effective permittivity of layered and continuously inhomogeneous dielectric spheres, J. Electromag. Waves Applic. **3**, 37 (1989).

[26] A. Sihvola and I. Lindell, Transmission line analogy for calculating the effective permittivity of mixtures with spherical multilayer scatterers, J. Electromagn. Waves Applic. **2**, 741 (1988).

[27] A. Sihvola and I. Lindell, Polarizability and effective permittivity of layered and continuously inhomogeneous dielectric ellipsoids, J. Electromagn. Waves Applic. **4**, 1 (1990).

[28] J. Keller, Conductivity of a medium containing a dense array of perfectly conducting spheres or cylinders or nonconducting cylinders, J. Appl. Phys. **34**, 991 (1963).

[29] A. Dykhne, Conductivity of a two-dimensional two-phase system, Sov. Phys. JETP **32**, 63 (1971).

[30] K. Mendelson, A theorem on the effective conductivity of a two-dimensional heterogeneous medium, J. Appl. Phys. **46**, 4740 (1975).

[31] J. A. Stratton, *Electromagnetic Theory* (John Wiley & Sons, Hoboken, New Jersey, 2007), Vol. 33.

[32] A. Sihvola, H. Kettunen, and H. Wallén, Mixtures and composite particles: Correspondence of effective description, in *Proceedings of the 2013 International Symposium on Electromagnetic Theory* (IEEE, Piscataway, NJ, 2013), pp. 908–911.

[33] J. Meixner, The behavior of electromagnetic fields at edges, IRE Trans. Antenn. Propag. **20**, 442 (1972).

[34] N. M. Estakhri and A. Alù, Physics of unbounded, broadband absorption/gain efficiency in plasmonic nanoparticles, Phys. Rev. B **87**, 205418 (2013).